



# Humidity sensing using THz metamaterial with silk protein fibroin

HWAN SIK KIM, SUNG HO CHA, BISWAJIT ROY, SUNGHWAN KIM, AND Y. H. AHN\*

*Department of Physics and Department of Energy Systems Research, Ajou University, Suwon 16499, South Korea*

\*[ahny@ajou.ac.kr](mailto:ahny@ajou.ac.kr)

**Abstract:** In this study, we developed hybrid humidity sensing methods by incorporating silk fibroin protein onto metamaterials, operating in the terahertz (THz) frequencies; the resonant frequency shifted but saturated at a specific thickness due to the limited sensing volume of the metamaterial. From the saturated value, we extracted the dielectric constant for the silk films. We also observed additional resonance shifts when we applied humid air to silk-coated metamaterials, due to the increased water molecule numbers on the film. Frequency shifts depend linearly on relative humidity. Also, in situ THz spectroscopy measurements reveal that the time response is instantaneous within our detection limit, especially upon exposure to humid air, whereas the small slowly decaying component appeared when we applied dry air. The time taken by the slow component in the drying process was 10–50 s, depending on film thickness. This could optimize humidity sensors as a fast and efficient detection tool to measure air humidity.

© 2018 Optical Society of America under the terms of the [OSA Open Access Publishing Agreement](#)

## 1. Introduction

Silk fibroin has attracted great attention for potential applications in which biocompatible materials are required because it is mechanically robust, harmless inside the body, optically transparent, and easy to fabricate; thus, it will enable the potential application of novel optical elements and biophotonic devices that could be implanted into the human body [1–8]. In particular, silk fibroin has been adopted as a transparent and flexible substrate for fabricating electronic and optoelectronic devices [9–12]. For instance, plasmonic and metamaterial patterns (which interact resonantly with electromagnetic waves) were successfully incorporated into the silk substrates, which serve as an efficient future platform for novel flexible optoelectronic devices. This would enable the fabrication of hybrid silk-based sensors that couple bio-functionality into the electromagnetic resonances that change in response to the local environment. In particular, the physical properties of silk fibroin are known to suffer a dramatic change when water molecules are absorbed; hence, humidity sensing has been demonstrated by monitoring the optical reflection spectra of silk films associated with its structural change [13,14].

On the other hand, metamaterials consist of a metallic structure that interacts with an incident electromagnetic wave and have great potential applications such as negative refraction, cloaking, super lensing, and sensitive sensing [15–18]. In particular, the metamaterial resonances are highly sensitive to changes in permittivity of the gap area, and hence, they are ideally suited for sensing dielectric materials [19–24]. For instance, we found that the metamaterials operating in the terahertz (THz) frequency range can be used as sensitive biosensors for the detection of low-density microorganisms [25–27]. This was possible because the detection volume is highly confined near the gap of the metamaterials. Specifically, the vertical range of the detection volume has been estimated to be several micrometers, depending on the geometry of the pattern; thus, it is highly desirable to use

metamaterials to address the permittivity of the thin films and liquids without requiring a large amount of the materials [23].

In this study, we developed a humidity sensing platform in which a small amount of silk fibroin proteins is incorporated into the THz metamaterials patterns. We first determined the dielectric constant of the fibroin film by measuring the frequency shift of the metamaterials as a function of the film thickness. By measuring the dielectric constant of the thin silk film, which is strongly influenced by water absorption, we can monitor the air humidity. We also measured in situ the time-response of the frequency shift and found the optimal conditions for humidity sensing.

## 2. Experimental results and discussion

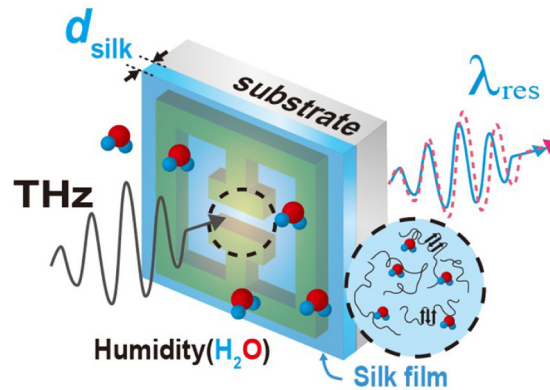


Fig. 1. Schematic of the hybrid THz humidity sensors. The silk fibroin film was deposited on the THz metamaterials.

A schematic of the THz hybrid metamaterial sensor for humidity detection is illustrated in Fig. 1 [23]. We first fabricated THz metamaterial patterns on a silicon substrate (resistivity  $> 10000 \Omega \cdot \text{cm}$  and a thickness of  $550 \mu\text{m}$ ), using a photolithography method, followed by metal evaporation of Cr/Au ( $2 \text{ nm}/98 \text{ nm}$ ). The THz metamaterials consisted of electrical split-ring resonators with a line width of  $4 \mu\text{m}$ , gap width of  $3 \mu\text{m}$ , side arm length of  $36 \mu\text{m}$ , and periodicity of  $50 \mu\text{m}$ . Silk fibroin solution was produced following previously reported protocols [28]. Briefly, the cocoons were boiled for 30 min in a 0.2-M solution of sodium carbonate to remove sericin. The fibers were dried overnight and then dissolved in a 9-M solution of lithium bromide. After a dialysis process, we finally obtained an aqueous solution of silk fibroin with a density of 71 mg/ml. We coated the silk films on the metamaterials by using the spin-coating method (for thin films less than 500 nm) or the drop-casting method (for the relatively thick films) from the aqueous solution with different densities of silk fibroin. THz transmission amplitudes of THz hybrid metamaterial devices were obtained from a conventional THz-TDS system. We monitored the change in the THz transmission through the sensors while varying the film thickness and humidity of the environment.

In general, metamaterials have a gap structure that works as a capacitor due to the charge accumulation when a circular current is generated by the incident wave [29]. As a result, inductive-capacitive ( $LC$ ) resonance appears in the metamaterials, which is mainly determined by geometrical parameters such as gap width, length of side arm, metal thickness, and substrate refractive index [30–33]. The  $LC$  resonance is sensitive to the changes in effective permittivity of the gap area as previously mentioned; hence, dielectric materials placed in the gap area modify the resonant frequency [23,25]. In this work, the silk film, whose dielectric constant varies with air humidity, functions as target materials for dielectric sensing.

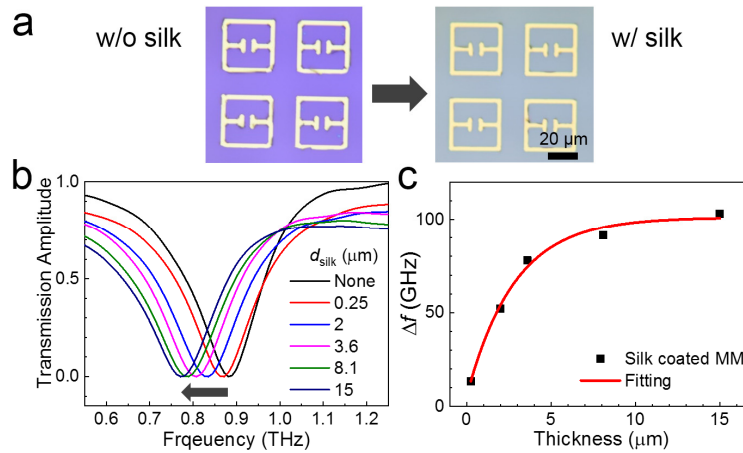


Fig. 2. (a) Microscopy image of the metamaterials before and after the deposition of a silk fibroin film with  $d_{\text{silk}} = 8.1 \mu\text{m}$ . (b) Transmission amplitudes for different silk film thickness from  $d_{\text{silk}} = 0 - 15 \mu\text{m}$ . (c) Plot of the frequency shift as a function of  $d_{\text{silk}}$  extracted from (b).

As we spin-coat (or drop-cast) the silk protein film onto the metamaterial, the resonant frequency shifts toward the red because of the change in the dielectric configuration of the gap area [23,25]. The microscopy images before and after the fibroin film coating (with thickness of  $8.1 \mu\text{m}$ ) are shown in Fig. 2(a), and the transmission spectra are plotted as a function of silk film thickness in Fig. 2(b). As expected, the resonant frequency shifts toward the red as we increase the film thickness. We plotted the frequency shift ( $\Delta f$ ) as a function of film thickness in Fig. 2(c). The parameter  $\Delta f$  increases with film thickness, but it exhibits saturation behavior, as found in previous studies [23]. Once the saturation condition is reached ( $d_{\text{silk}} > 10 \mu\text{m}$ ), we can measure the dielectric constant consistently without the knowledge of the specimen amount or film thickness. This allows us to measure the dielectric constants ( $\epsilon_r$ ) accurately while using very small amounts of the target material, as compared to conventional transmission methods requiring large amounts of specimens. From the explicit relation between the saturated frequency ( $\Delta f_{\text{sat}}$ ) and  $\epsilon_r$ , i.e.,  $\Delta f_{\text{sat}} / f_0 = \alpha(\epsilon_r - \epsilon_{\text{air}}) / \epsilon_{\text{eff}}$ , where  $f_0$  is the resonant frequency without silk,  $\alpha$  is the coefficient,  $\epsilon_{\text{eff}}$  is the effective dielectric constant of the substrate, and  $\epsilon_{\text{air}}$  is the air dielectric constant, we obtained  $\epsilon_r = 4.31$  (refractive index of 2.08). Here, we used  $\alpha = 0.1886$  and  $\epsilon_{\text{eff}} = 5.52$ , as found in the literature [23]. The measured refractive index was slightly higher than the previously reported value of  $n = 1.91$  [9].

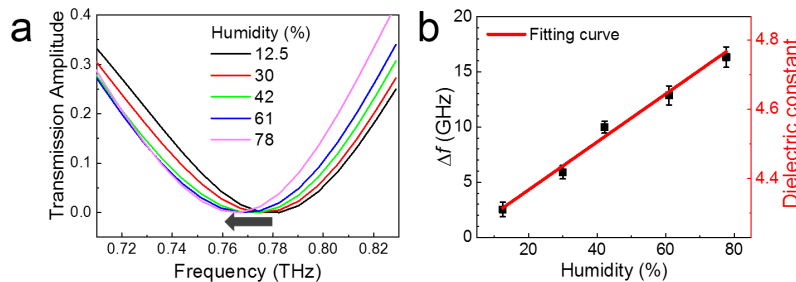


Fig. 3. (a) Transmission amplitude for different humidity conditions from 12.5 – 78% for  $d_{\text{silk}} = 15 \mu\text{m}$ . (b) Frequency shift as a function of humidity, extracted from (a).

Figure 3(a) shows the transmission spectra of the silk-coated metamaterial device (with a thickness of 15  $\mu\text{m}$ ) for different relative humidities (RH) from 12.5 – 78%. We used a home-built humidifier in which we can control the humidity by mixing the nitrogen with the gas from the conventional humidifier. The humid air was supplied into an acrylic box with dimensions 6.5 cm  $\times$  5.5 cm  $\times$  8 cm, containing the hybrid silk device for the THz transmission experiment. The reference humidity was measured by a commercial humidity sensor (Testo SE & Co. KGaA, testo 605-H1). As we increase humidity, the resonant frequency shifts toward the red, which indicates that the dielectric constant increases further as the humidity increases. It has been inferred that a high humidity induces the infiltration of the water molecule into the silk fibers by binding themselves to the random coils within the amorphous region of silk, disrupting the relatively weak hydrogen bonding [13,14]. Because the THz dielectric constant of water ( $\epsilon_r = 4.9$ ) is much higher than the fibroin film, increasing water content will boost the dielectric constant of the film [34].

The resonant frequency shift increases linearly with an increase in humidity, from 2.5 GHz to 16.3 GHz, with the dielectric constants varying from 4.31 to 4.75, as shown in Fig. 3(b). Therefore, the silk hybrid sensor works nicely as a sensitivity humidity sensor by monitoring the humidity-dependent dielectric constant of the thin silk film. From the fitting curve, the sensitivity in terms of  $\Delta f/\text{RH}$  reaches 0.22 GHz/%. Because the elaborate fitting procedure allows a frequency shift resolution as small as 0.5 GHz, we are able to identify an RH change of  $\sim 2.3\%$ , which is within the sensitivity of our humidity sensors, used as reference. Typically, a cost-effective commercial sensor has an RH sensitivity of 5%, whereas a sensitivity as good as 1% is also available in the market. Recently, enhanced sensitivity has been achieved by utilizing the hybrid devices such as the infrared photonic crystal cavity coated with humidity-sensitive materials [35–37]. Likewise, our sensitivity could be improved further by simply improving the Q-factor and the signal-to-noise ratio of the THz spectroscopy systems, or by increasing the measurement time.

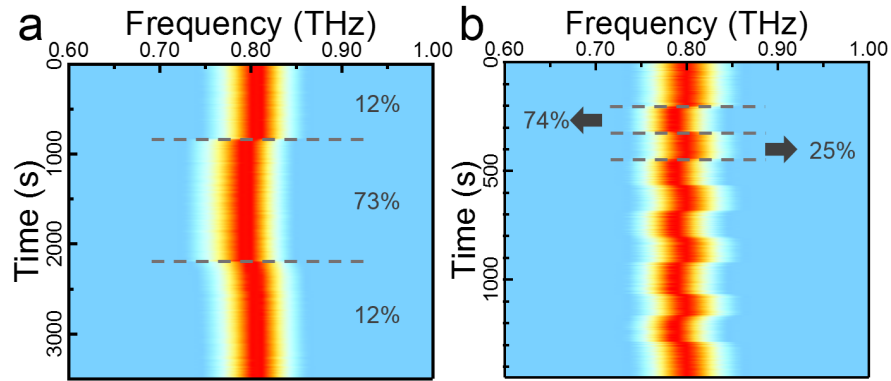


Fig. 4. (a) In situ THz spectroscopy results recorded for THz transmission as a function of spectrum (x-axis) and time (y-axis) with  $d_{\text{silk}} = 3.6 \mu\text{m}$ . Initially, the humidity was measured at 12% and we applied humid air with 73% humidity for 23 min. (b) In situ THz spectroscopy results when the humidity was changed from 25% and 74% repeatedly ( $d_{\text{silk}} = 3.9 \mu\text{m}$ ).

To address the time-response of the humidity sensing, we performed in situ THz spectroscopy as shown by the representative image in Fig. 4(a), with a time interval of 4 s [38]. The thickness of the fibroin film was 3.6  $\mu\text{m}$  (with a RMS deviation of 0.6 GHz). Here, we measured the THz transmission as a function of both the spectrum (x-axis) and measurement time (y-axis), while we varied the humidity. Initially, the resonant peak ( $f$ ) was located at  $f = 0.807$  THz for dry air condition (12%). The resonance frequency position remained stationary over 10 min. As we abruptly increase the humidity to 73%, the frequency shift shows an abrupt redshift to  $f = 0.795$  THz (i.e.,  $\Delta f = 12$  GHz). It returned to its original

value as we change the humidity back to dry air condition. Because the sensor was reset with a relatively sharp response without noticeably demonstrating the hysteresis effect with respect to the humidity change, the silk-based hybrid sensor was capable of repeating the operation when we changed the humidity repeatedly as shown in Fig. 4(b). In addition, we could not observe humidity-induced damage in the silk film over the course of measurements. This is because the water infiltration induces the de-bonding of hydrogen bonds between fibroin polymers and subsequent water evaporation does not change the intrinsic molecular structure of the polymers [14]. Interestingly, the sensitivity tends to decrease with an increase in the film crystallinity (e.g., after vacuum treatment for 24 hr). This is because the silk crystalline region contains densely arranged  $\beta$ -sheet macromolecular chains, which prevents water infiltration [14].

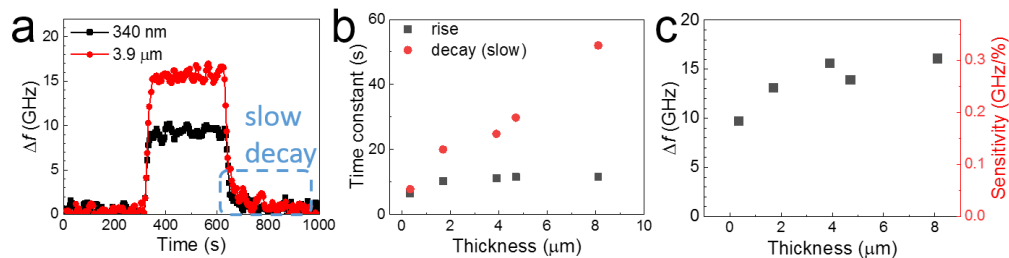


Fig. 5. (a) Frequency shift as a function of time extracted from in situ THz spectroscopy for  $d_{\text{silk}} = 340$  nm (black) and 3.9  $\mu\text{m}$  (red). (b) Plot of the rise (black) and decay (red) time constants as a function of  $d_{\text{silk}}$ . (c) Plot of the maximum frequency shift as a function of film thickness.

To investigate the dynamical behaviors of the humidity dependent frequency shift in detail, we plotted the frequency shift as a function of time in Fig. 5(a) for two silk film thickness of 340 nm (black) and 3.9  $\mu\text{m}$  (red). As mentioned before, the time response is characterized by sharp rise and decay times that are limited by our detection speed ( $\sim 4$  s) as we turn on and off the humid air. However, we found that there is a slow decay component extending over tens of seconds, as indicated by a blue dashed box. The origin for the slow component associated with the drying process is the length of time it takes for the water molecule to escape from the random coil [13,14]. In Fig. 5(b), we plotted the slow component in decay time constant (red) as a function of film thickness. The plot of the rise time constant (black) is shown together for comparison, which yields  $\sim 10$  s regardless of the thickness. Clearly, the slow decay component increases with silk thickness, implying that it takes more time for the water molecule to escape from the thick films. Therefore, for a fast response, it is desirable to use the thin fibroin film. For instance, the slow time constant was measured to be 7.8 s for  $d_{\text{silk}} = 340$  nm, as compared to 52 s for  $d_{\text{silk}} = 8.1$   $\mu\text{m}$ . Surprisingly, the amount of the frequency shift was not influenced significantly by the thickness (9.7 GHz for  $d_{\text{silk}} = 340$  nm, compared to 16.1 GHz for  $d_{\text{silk}} = 8.1$   $\mu\text{m}$ ) as shown in Fig. 5(c). The corresponding sensitivity value ranges from 0.18 GHz/% to 0.30 GHz/%. This is likely because the effect of the water molecule absorption was localized near the surface of the silk film ( $< 1$   $\mu\text{m}$ ) over the course of our experiment ( $\sim 1$  hr). In addition, the unexpectedly high sensitivity for the films with  $d_{\text{silk}} = 340$  nm can be attributed to the humidity-induced increase in the film thickness [14]. We also emphasize that the sharp time response was possible because the THz metamaterial allows us to use very thin silk layer because its detection volume is strongly localized near the surface. Our work will provide very useful information in the development and optimization of advanced hybrid humidity sensors and can be extended for the future development of advanced biological, chemical, and environmental sensors.

### 3. Conclusion

In conclusion, we measured the humidity-dependent dielectric constant of silk film by coating a small amount of silk fibroin protein onto THz metamaterials. As we deposit the silk film onto a metamaterial, the resonant frequency shifts but saturates at a specific thickness ( $> 10 \mu\text{m}$ ) due to the limited sensing volume of the metamaterial. From the saturated value, we extracted the dielectric constant of silk films, yielding  $\epsilon_r = 4.31$  (refractive index of 2.08). Importantly, we observed additional resonance shifts when we applied humid air to silk-coated metamaterials, due to the increased content of water molecules in the film. The frequency shift depends linearly on the humidity, reaching  $\epsilon_r = 4.75$  at 78% relative humidity. The sensitivity in terms of  $\Delta f/\text{RH}$  reaches 0.22 GHz/%, with which we are able to identify an RH change of  $\sim 2.3\%$ . In addition, in situ THz spectroscopy reveals an instantaneous time response within our detection limit of a couple of seconds, whereas the slowly decaying component appeared when we dried the air. The slow component in the drying process reaches 10–50 s, depending on the film thickness; hence, the use of thin silk film is critical for the fast time-response. As a result, the hybrid silk-metamaterial sensors allow us to develop fast, sensitive, and low-cost humidity sensors. Future investigation is required to optimize the devices further by introducing a new design of metamaterials with high-Q factors, high-speed THz measurement tools, and potential, by engineering the chemical properties of silk fibroin proteins.

### Funding

National Research Foundation of Korea (NRF) (2017R1A2B4009177); Korea Institute of Energy Technology Evaluation and Planning (KETEP) (20164030201380)

### References

1. C. Jiang, X. Wang, R. Gunawidjaja, Y. H. Lin, M. K. Gupta, D. L. Kaplan, R. R. Naik, and V. V. Tsukruk, "Mechanical properties of robust ultrathin silk fibroin films," *Adv. Funct. Mater.* **17**(13), 2229–2237 (2007).
2. H. Perry, A. Gopinath, D. L. Kaplan, L. D. Negro, and F. G. Omenetto, "Nano- and micropatterning of optically transparent, mechanically robust, biocompatible silk fibroin films," *Adv. Mater.* **20**(16), 3070–3072 (2008).
3. D. H. Kim, J. Viventi, J. J. Amsden, J. Xiao, L. Vigeland, Y. S. Kim, J. A. Blanco, B. Panilaitis, E. S. Frechette, D. Contreras, D. L. Kaplan, F. G. Omenetto, Y. Huang, K. C. Hwang, M. R. Zakin, B. Litt, and J. A. Rogers, "Dissolvable films of silk fibroin for ultrathin conformal bio-integrated electronics," *Nat. Mater.* **9**(6), 511–517 (2010).
4. H. Tao, D. L. Kaplan, and F. G. Omenetto, "Silk materials-A road to sustainable high technology," *Adv. Mater.* **24**(21), 2824–2837 (2012).
5. S. W. Hwang, H. Tao, D. H. Kim, H. Cheng, J. K. Song, E. Rill, M. A. Brenckle, B. Panilaitis, S. M. Won, Y. S. Kim, Y. M. Song, K. J. Yu, A. Ameen, R. Li, Y. Su, M. Yang, D. L. Kaplan, M. R. Zakin, M. J. Slepian, Y. Huang, F. G. Omenetto, and J. A. Rogers, "A physically transient form of silicon electronics," *Science* **337**(6102), 1640–1644 (2012).
6. S. Kim, A. N. Mitropoulos, J. D. Spitzberg, H. Tao, D. L. Kaplan, and F. G. Omenetto, "Silk inverse opals," *Nat. Photonics* **6**(12), 818–823 (2012).
7. M. Lee, H. Jeon, and S. Kim, "A highly tunable and fully biocompatible silk nanoplasmonic optical sensor," *Nano Lett.* **15**(5), 3358–3363 (2015).
8. B. Zhu, H. Wang, W. R. Leow, Y. Cai, X. J. Loh, M. Y. Han, and X. Chen, "Silk Fibroin for Flexible Electronic Devices," *Adv. Mater.* **28**(22), 4250–4265 (2016).
9. H. Tao, J. J. Amsden, A. C. Strikwerda, K. Fan, D. L. Kaplan, X. Zhang, R. D. Averitt, and F. G. Omenetto, "Metamaterial silk composites at terahertz frequencies," *Adv. Mater.* **22**(32), 3527–3531 (2010).
10. H. Tao, M. A. Brenckle, M. Yang, J. Zhang, M. Liu, S. M. Siebert, R. D. Averitt, M. S. Manno, M. C. McAlpine, J. A. Rogers, D. L. Kaplan, and F. G. Omenetto, "Silk-based conformal, adhesive, edible food sensors," *Adv. Mater.* **24**(8), 1067–1072 (2012).
11. B. Li, G. Xiao, F. Liu, Y. Qiao, C. M. Li, and Z. Lu, "A flexible humidity sensor based on silk fabrics for human respiration monitoring," *J. Mater. Chem. C Mater. Opt. Electron. Devices* **6**(16), 4549–4554 (2018).
12. M. Jo, K. Min, B. Roy, S. Kim, S. Lee, J. Y. Park, and S. Kim, "Protein-Based Electronic Skin Akin to Biological Tissues," *ACS Nano* **12**(6), 5637–5645 (2018).
13. Y. Y. Diao, X. Y. Liu, G. W. Toh, L. Shi, and J. Zi, "Multiple structural coloring of silk-fibroin photonic crystals and humidity-responsive color sensing," *Adv. Funct. Mater.* **23**(43), 5373–5380 (2013).
14. Q. Li, N. Qi, Y. Peng, Y. Zhang, L. Shi, X. Zhang, Y. Lai, K. Wei, I. S. Kim, and K. Q. Zhang, "Sub-micron silk fibroin film with high humidity sensibility through color changing," *RSC Advances* **7**(29), 17889–17897 (2017).

15. J. B. Pendry, A. J. Holden, D. J. Robbins, and W. J. Stewart, "Magnetism from conductors and enhanced nonlinear phenomena," *IEEE Trans. Microw. Theory Tech.* **47**(11), 2075–2084 (1999).
16. R. A. Shelby, D. R. Smith, and S. Schultz, "Experimental verification of a negative index of refraction," *Science* **292**(5514), 77–79 (2001).
17. J. B. Pendry, D. Schurig, and D. R. Smith, "Controlling electromagnetic fields," *Science* **312**(5781), 1780–1782 (2006).
18. J. F. O'Hara, R. Singh, I. Brener, E. Smirnova, J. Han, A. J. Taylor, and W. Zhang, "Thin-film sensing with planar terahertz metamaterials: Sensitivity and limitations," *Opt. Express* **16**(3), 1786–1795 (2008).
19. T. Driscoll, G. O. Andreev, D. N. Basov, S. Palit, S. Y. Cho, N. M. Jokerst, and D. R. Smith, "Tuned permeability in terahertz split-ring resonators for devices and sensors," *Appl. Phys. Lett.* **91**(6), 062511 (2007).
20. H. J. Lee and J. G. Yook, "Biosensing using split-ring resonators at microwave regime," *Appl. Phys. Lett.* **92**(25), 254103 (2008).
21. H. Tao, A. C. Strikwerda, M. Liu, J. P. Mondia, E. Ekmekci, K. Fan, D. L. Kaplan, W. J. Padilla, X. Zhang, R. D. Averitt, and F. G. Omenetto, "Performance enhancement of terahertz metamaterials on ultrathin substrates for sensing applications," *Appl. Phys. Lett.* **97**(26), 261909 (2010).
22. M. Labidi, J. B. Tahar, and F. Choubani, "Meta-materials applications in thin-film sensing and sensing liquids properties," *Opt. Express* **19**(S4), A733–A739 (2011).
23. S. J. Park, S. A. N. Yoon, and Y. H. Ahn, "Dielectric constant measurements of thin films and liquids using terahertz metamaterials," *RSC Advances* **6**(73), 69381–69386 (2016).
24. I. Al-Naib, "Biomedical Sensing with Conductively Coupled Terahertz Metamaterial Resonators," *IEEE J. Sel. Top. Quantum Electron.* **23**(4), 4700405 (2017).
25. S. J. Park, J. T. Hong, S. J. Choi, H. S. Kim, W. K. Park, S. T. Han, J. Y. Park, S. Lee, D. S. Kim, and Y. H. Ahn, "Detection of microorganisms using terahertz metamaterials," *Sci. Rep.* **4**(1), 4988 (2015).
26. S. J. Park, B. H. Son, S. J. Choi, H. S. Kim, and Y. H. Ahn, "Sensitive detection of yeast using terahertz slot antennas," *Opt. Express* **22**(25), 30467–30472 (2014).
27. S. J. Park, S. H. Cha, G. A. Shin, and Y. H. Ahn, "Sensing viruses using terahertz nano-gap metamaterials," *Biomed. Opt. Express* **8**(8), 3551–3558 (2017).
28. F. G. Omenetto and D. L. Kaplan, "New opportunities for an ancient material," *Science* **329**(5991), 528–531 (2010).
29. H. T. Chen, W. J. Padilla, J. M. O. Zide, A. C. Gossard, A. J. Taylor, and R. D. Averitt, "Active terahertz metamaterial devices," *Nature* **444**(7119), 597–600 (2006).
30. C. Rockstuhl, T. Zentgraf, H. Guo, N. Liu, C. Etrich, I. Loa, K. Syassen, J. Kuhl, F. Lederer, and H. Giessen, "Resonances of split-ring resonator metamaterials in the near infrared," *Appl. Phys. B* **84**(1-2), 219–227 (2006).
31. A. K. Azad, A. J. Taylor, E. Smirnova, and J. F. O'Hara, "Characterization and analysis of terahertz metamaterials based on rectangular split-ring resonators," *Appl. Phys. Lett.* **92**(1), 011119 (2008).
32. D. J. Park, J. T. Hong, J. K. Park, S. B. Choi, B. H. Son, F. Rotermund, S. Lee, K. J. Ahn, D. S. Kim, and Y. H. Ahn, "Resonant transmission of terahertz waves through metallic slot antennas on various dielectric substrates," *Curr. Appl. Phys.* **13**(4), 753–757 (2013).
33. D. J. Park, S. J. Park, I. Park, and Y. H. Ahn, "Dielectric substrate effect on the metamaterial resonances in terahertz frequency range," *Curr. Appl. Phys.* **14**(4), 570–574 (2014).
34. C. Rønne, L. Thrane, P. O. Åstrand, A. Wallqvist, K. V. Mikkelsen, and S. R. Keiding, "Investigation of the temperature dependence of dielectric relaxation in liquid water by THz reflection spectroscopy and molecular dynamics simulation," *J. Chem. Phys.* **107**, 5319–5331 (1997).
35. S. A. Kolpakov, N. T. Gordon, C. Mou, and K. Zhou, "Toward a new generation of photonic humidity sensors," *Sensors (Basel)* **14**(3), 3986–4013 (2014).
36. C. Zhao, Q. Yuan, L. Fang, X. Gan, and J. Zhao, "High-performance humidity sensor based on a polyvinyl alcohol-coated photonic crystal cavity," *Opt. Lett.* **41**(23), 5515–5518 (2016).
37. X. Gan, C. Zhao, Q. Yuan, L. Fang, Y. Li, J. Yin, X. Ma, and J. Zhao, "High performance graphene oxide-based humidity sensor integrated on a photonic crystal cavity," *Appl. Phys. Lett.* **110**(15), 151107 (2017).
38. S. J. Park, A. R. Kim, J. T. Hong, J. Y. Park, S. Lee, and Y. H. Ahn, "Crystallization kinetics of lead halide perovskite film monitored by in situ terahertz spectroscopy," *J. Phys. Chem. Lett.* **8**(2), 401–406 (2017).